

SUPPLEMENTAL DATA

'Cold Finger' Target Assembly

The smaller 'cold finger' target is illustrated in Supplemental Figure 1. A recirculating chilled water circuit cooled the entire target assembly and did not need to be purged to load or retrieve the target plate. The target plate was exposed to a continuous flow of helium used to cool the niobium vacuum separation foil. After irradiation, the target plate was readily dislodged from the target holder via a pneumatic actuator, causing it to drop, with guidance from a plastic funnel, into a shielded container. Because the ACSI cyclotron has partial shields covering the target selectors, the target plate could be manually retrieved with minimal radiation exposure to the cyclotron staff.

'Large Target' Station

The large target station is illustrated in Supplemental Figure 2. This target station was made almost entirely of aluminum parts to minimize activation, and avoided as much as possible the use of seals and fittings that could be subject to degradation in high neutron and gamma fields. The target station had a stray beam detector and four adjustable beam collimators (top, bottom, left, right) to ensure the high beam power is appropriately distributed across the target plate. The target plate was held in an aluminum capsule with passages for cooling water to flow over the back of the target plate. The target station assembly incorporated pneumatic actuators that locked the capsule to the target station to allow the interior of the capsule to be sealed to a vacuum environment, while cooling water was delivered through the back-end of the assembly. The complete beam line, target and shield assembly is shown in Supplemental Figure 2.

The target capsule was inserted and retrieved from the target station through a smooth walled flexible tube sealed to the radiochemistry hot cell (Comecer MIP-1390) and directly connected to the target station(1). The capsule was moved by a custom-designed, motor-driven, mechanical tape

drive system employing 1/16" x 1/8" spring steel wire. The target capsule was pushed through the transfer tube from the hot cell to the target station until mechanical sensors detected the capsule at the destination. Upon activation of the sensors, pneumatic actuators in the target station slid and locked the target capsule in place. The target station was brought under rough vacuum and the vacuum isolation valve opened to the beam line vacuum. The water-cooling circuit was activated before irradiation.

The proton beam was adjusted for optimal distribution over the molybdenum layer deposited on the target plate, in both the long and short axis of the target plate. The beam profile, measured from the density of a radiographic film exposed to an irradiated target plate, is shown in Supplemental Figure 4.

Target retrieval was accomplished by isolating the target station from the beam line vacuum, venting to atmospheric pressure, stopping the water flow, followed by purging any residual water from the target capsule cooling channels. The tape drive was then driven from the radiochemistry hot cell, through the transfer tube, until the mechanical locking device engaged with the target capsule. The pneumatic actuators holding the target capsule in place were then de-activated and the capsule pulled back to the radiochemistry hot cell.

Large Target Dissolution Procedure

For the large area targets, once the target capsule was recovered in the hot cells, telemanipulator arms (Tru-Motion Products) were used to pick up the capsule and insert it into a target dissolution base, thus using the target capsule to form a dissolution chamber. This aluminum base was designed with two 1/8" apertures to flow liquid from the base to the top of the target plate. A long rigid polyether ether ketone (PEEK) line extended from the base to the upper portion of the target capsule to vent the evolved gases and recover the liquid reaching the top of the capsule.

A simple apparatus consisting of a peristaltic pump and three-way valves was used to move 45 mL of 30% H₂O₂ solution. The target capsule was filled with H₂O₂ at a flow rate of 3-4.5 mL/min over a period of 10-15 min.

The H₂O₂ was left in the capsule for 20 minutes and slowly recirculated for another 10 min to ensure complete dissolution of the molybdenum layer. The capsule was then emptied by reversing the peristaltic pump direction to a second vessel. The target solution was evaporated to dryness, and the resulting powder dissolved in 4M NaOH before purification. A picture of a target plate after dissolution is shown in Supplemental Figure 5.

Supplemental Table 1. Percentage of technetium radionuclides observed

Isotope	T _{1/2} (h)	Run 1	Run 2	Run 3	Run 4
Tc99m	6.02	99.66 ± 0.12%	99.52 ± 0.07%	99.91 ± 0.07%	99.78 ± 0.03%
Tc97m	2194	*	0.0014 ± 0.0001%	0.0135 ± 0.0006%	0.0082 ± 0.0004%
Tc96m	0.863	*	*	*	*
Tc96g	102.7	0.015 ± 0.002%	0.021 ± 0.001%	0.0035 ± 0.0003%	0.0069 ± 0.0003%
Tc95m	1464	*	<0.00001%	0.000108 ± 0.000003%	0.000178 ± 0.000004%
Tc95g	20	0.094 ± 0.004%	*	0.0128 ± 0.0009%	0.0375 ± 0.0015%
Tc94m	0.87	0.04 ± 0.12%	0.28 ± 0.07%	0.05 ± 0.07%	0.09 ± 0.03%
Tc94g	4.88	0.103 ± 0.004%	0.104 ± 0.005%	0.011 ± 0.002%	0.041 ± 0.002%
Tc93m	0.73	*	*	*	*
Tc93g	2.75	0.093 ± 0.007%	0.073 ± 0.009%	*	0.032 ± 0.004%

The numbers represent the percentage of all technetium species present at end-of-beam, with the measurement uncertainty.

The run numbers correspond to the experiments reported on Table 3 of the article.

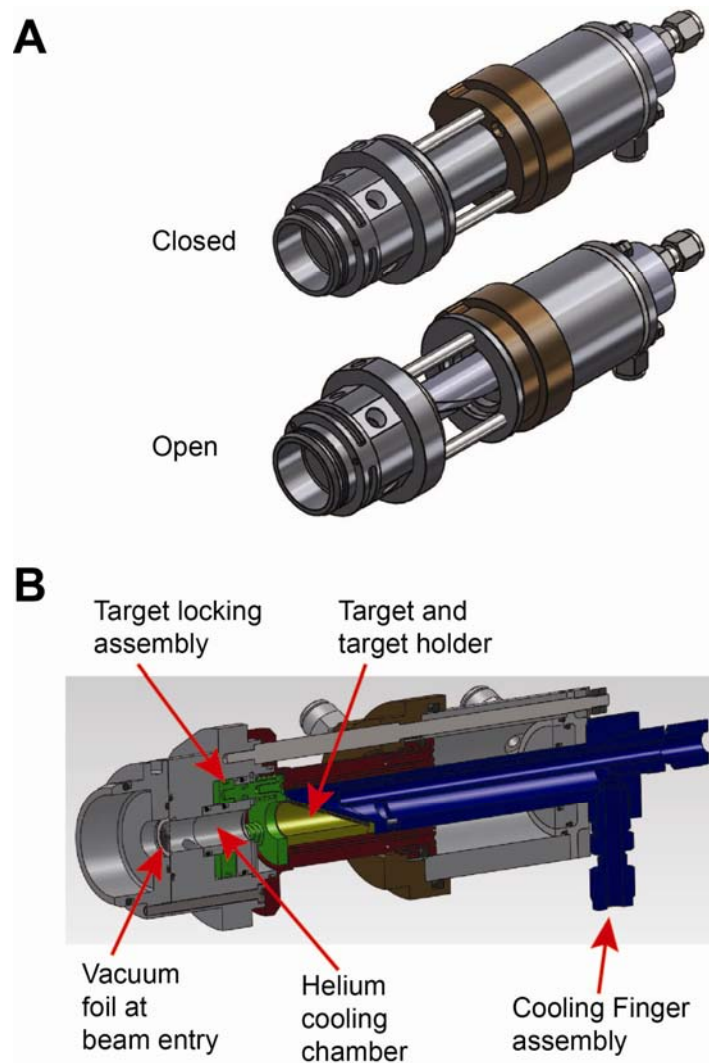
*Below minimal detectable activity.

Supplemental Table 2. Percentage of all radioisotopes

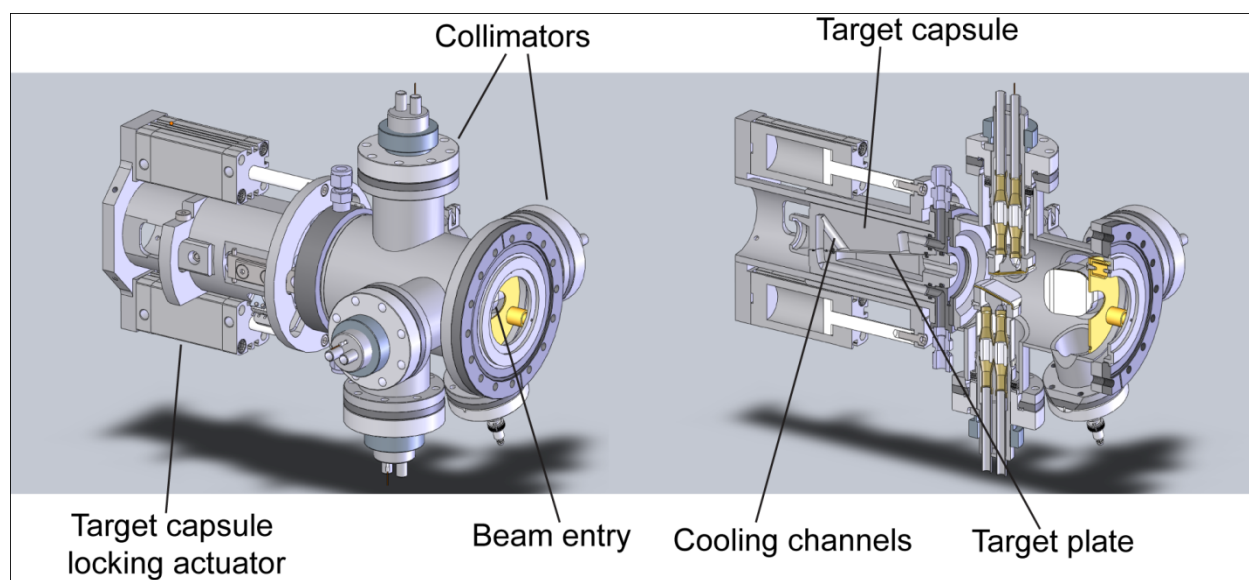
Isotope	T _{1/2} (h)	Run 1	Run 2	Run 3	Run 4
Tc99m	6.02	93.37 ± 0.16%	95.62 ± 0.10%	94.29 ± 0.12%	94.66 ± 0.09%
All other Tc	-	0.24 ± 0.11%	0.39 ± 0.07%	0.08 ± 0.06%	0.21 ± 0.03%
Mo99	65.9	1.21 ± 0.04%	1.23 ± 0.03%	1.83 ± 0.04%	1.82 ± 0.04%
Nb97	1.2	4.70 ± 0.11%	2.18 ± 0.06%	3.60 ± 0.09%	2.54 ± 0.08%
Nb96	23.4	0.071 ± 0.003%	0.045 ± 0.002%	0.107 ± 0.001%	0.130 ± 0.002%
Nb95m	86.4	*	*	*	*
Nb95	840	*	0.000112 ± 0.000005%	0.00078 ± 0.00002%	0.00071 ± 0.00002%

The numbers represent the percentage of all radioisotopes detected at end-of-beam, with the measurement uncertainty.

*Below minimal detectable activity.



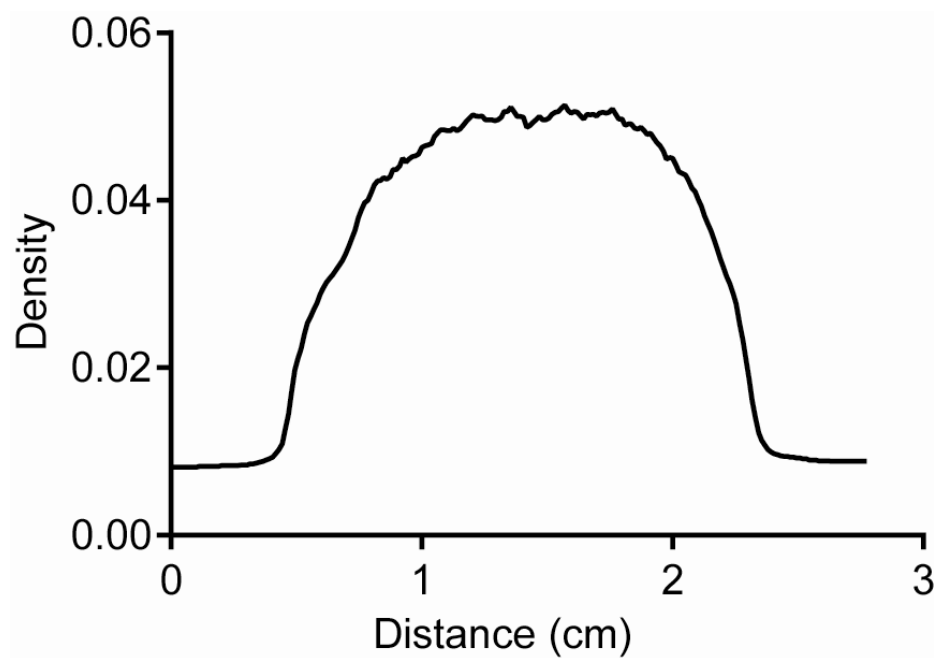
Supplemental Figure 1. External overview and cross-sectional view of the cold finger target. Irradiated target plates can be remotely dropped into a shielding container.



Supplemental Figure 2. External overview and cross-sectional view of the large target station. A target capsule is inserted mechanically from the left and locked in place by pneumatic actuators to seal the capsule in place and connect the cooling channels.



Supplemental Figure 3. Picture of the beam line, target station and associated shielding. The target abuts a concrete wall to improve neutron shielding. A moveable shield on rails is used to provide additional local shielding. The target capsule is automatically and remotely retrieved from the bottom of the target station.



Supplemental Figure 4. This figure shows the density profile measured across the short axis of a film exposed to an irradiated target backing plate. This was used to demonstrate the proton beam distribution over the target area (6 x 2.3 cm).



Supplemental Figure 5. Tantalum target plate after dissolution of the molybdenum layer by 30% hydrogen peroxide. Note the complete removal of the target material. The tantalum plate is reusable to prepare additional targets.

Supplemental References

1. Klug J, Buckley KR, Zeisler SK, et al. A New Transfer System for Solid Targets. *AIP Conf Proc.* 2012;1509:146-151.